

New Phytologist Supporting Information

Article title: A global phylogenetic regionalisation of vascular plants reveals a deep split between Gondwanan and Laurasian biotas

Angelino Carta^{1,2*}, Lorenzo Peruzzi^{1,2}, Santiago Ramírez-Barahona³

¹Unità di Botanica, Dipartimento di Biologia, Università di Pisa, 56126, Pisa, Italy

²Centro Interuniversitario per la Biodiversità Vegetale Big Data - PLANT DATA, Dipartimento di Scienze Biologiche, Geologiche e Ambientali, Alma Mater Studiorum Università di Bologna, 40126 Bologna, Italy

³Departamento de Botánica, Instituto de Biología, Universidad Nacional Autónoma de México (UNAM), Circuito Exterior s/n, Ciudad de México, 04510, Mexico

Article acceptance date: 28 October 2021

The following Supporting Information is available for this article:

Table S1. Total number of species of vascular plants used in the delimitation of phytogeographical units across the globe. Numbers for species with geographic and phylogenetic data or with only geographic data are reported, along with estimates of taxonomic completeness for each family. Estimations as from Plants of the World Online and the Pteridophyte Phylogeny Group for ferns, and Angiosperm Phylogeny Website Boraginales and Santalales.

Table S2. Performance of clustering algorithms (cophenetic correlation coefficient) for phylogenetic beta diversity ($p\beta_{sim}$) and beta diversity (β_{sim}) of global vascular species data.

Figure S1. Species richness and number of occurrences across 200 × 200 km grid cells.

Figure S2. Map of the terrestrial phylogenetically distinct phytogeographic units of the world constraining the number of clusters to $k = 3$.

Figure S3. Map of the terrestrial phylogenetically distinct phytogeographic units of the world constraining the number of clusters to $k = 4$.

Figure S4. Map of the terrestrial phylogenetically distinct phytogeographic units of the world constraining the number of clusters to $k = 5$.

Figure S5. Map of the terrestrial phylogenetically distinct phytogeographic units of the world constraining the number of clusters to $k = 6$.

Figure S6. Map of the terrestrial taxonomically distinct phytogeographic units of the world.

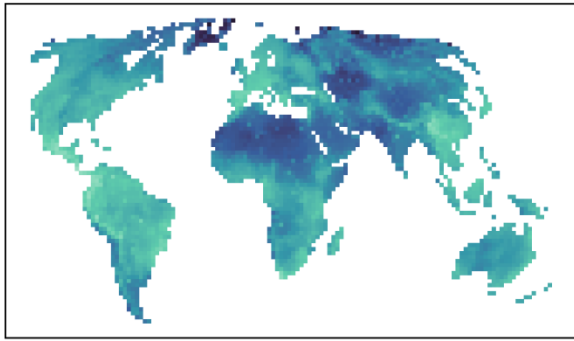
Figure S7. Maps of the terrestrial phylogenetic and taxonomic regionalisation of the world side by side.

Figure S8. Evolutionary distinctiveness within the 16 phytogeographical units, considering only lycophytes and ferns (a) and gymnosperms (b).

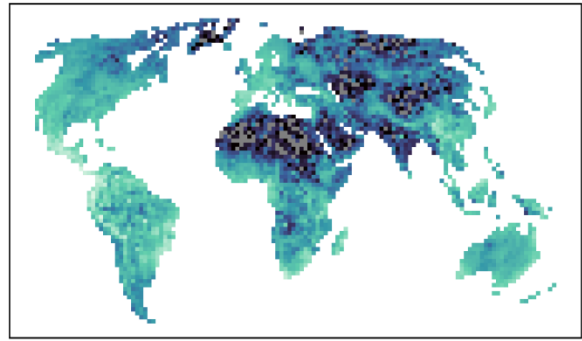
Table S2. Performance of clustering algorithms (cophenetic correlation coefficient) for phylogenetic beta diversity ($p\beta_{sim}$) and beta diversity (β_{sim}) of global vascular species data.

Linkage algorithm	$p\beta_{sim}$	β_{sim}
UPGMA agglomerative clustering method = "average"	0.661	0.808
Single linkage agglomerative clustering method = "single"	0.278	0.375
Complete linkage agglomerative clustering method = "complete"	0.532	0.489
Ward's minimum variance clustering method = "ward"	0.509	0.571
WPGMA agglomerative clustering method = "mcquitty"	0.552	0.590
WPGMC agglomerative clustering method = "median"	0.596	0.726
UPGMC agglomerative clustering method = "centroid"	0.484	0.281

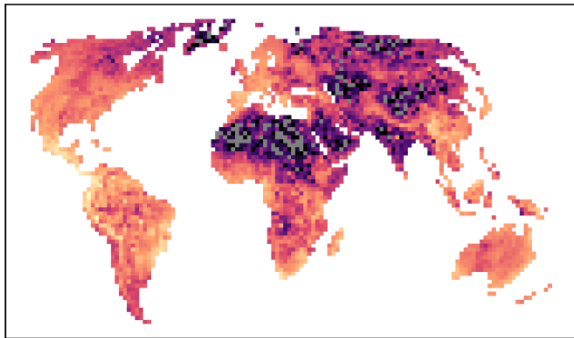
Estimate from ranges



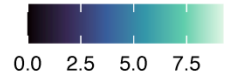
Estimate from occurrences



Unique occurrences per cell/species



Species richness (log)



Number of occurrences (log)

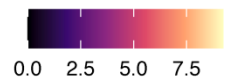


Figure S1. Species richness and number of occurrences across 200×200 km grid cells.

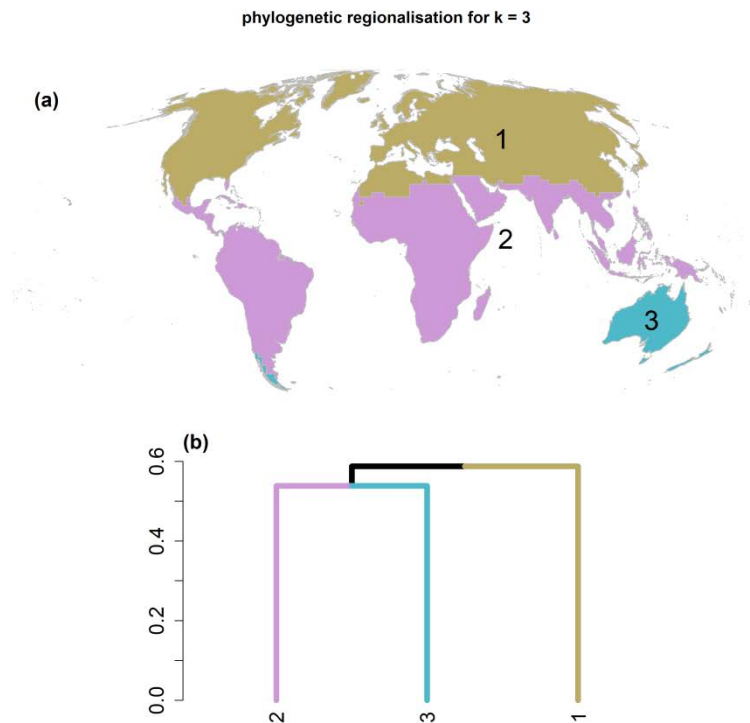


Figure S2. Map of the terrestrial phylogenetically distinct phytogeographic units of the world (a), and their relationship presented as a dendrogram of dissimilarity (b), as delimited by UPGMA hierarchical clustering of phylogenetic beta diversity ($p\beta_{sim}$) in 200×200 km grid cells, constraining the number of clusters to $k = 3$.

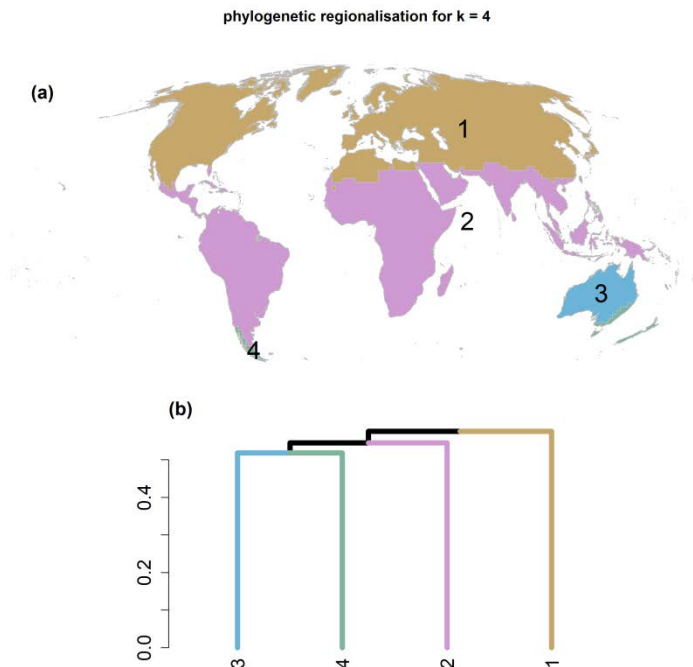


Figure S3. Map of the terrestrial phylogenetically distinct phytogeographic units of the world (a), and their relationship presented as a dendrogram of dissimilarity (b), as delimited by UPGMA hierarchical clustering of phylogenetic beta diversity ($p\beta_{sim}$) in 200×200 km grid cells, constraining the number of clusters to $k = 4$.

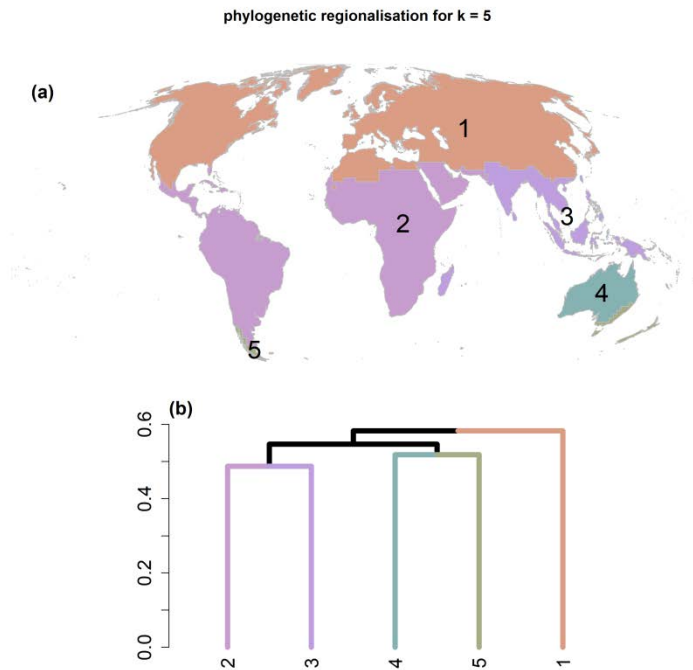


Figure S4. Map of the terrestrial phylogenetically distinct phylogeographic units of the world (a), and their relationship presented as a dendrogram of dissimilarity (b), as delimited by UPGMA hierarchical clustering of phylogenetic beta diversity ($p\beta_{sim}$) in 200×200 km grid cells, constraining the number of clusters to $k = 5$.

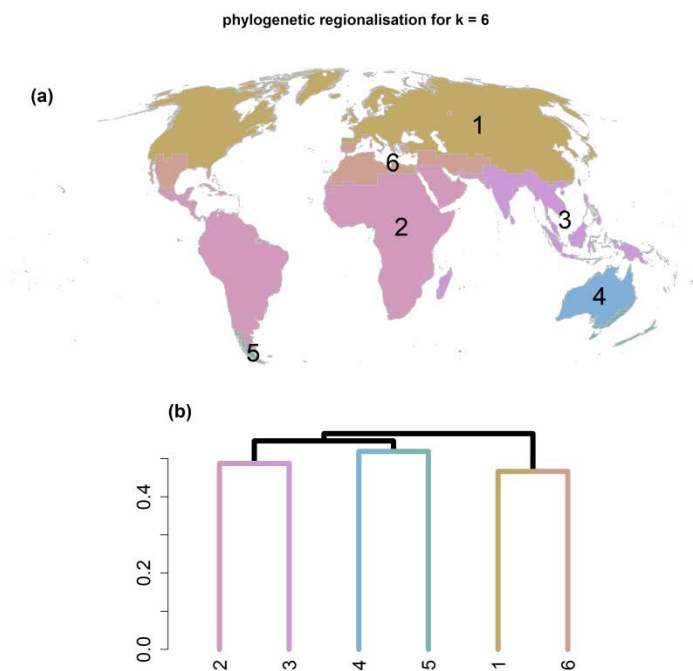


Figure S5. Map of the terrestrial phylogenetically distinct phylogeographic units of the world (a), and their relationship presented as a dendrogram of dissimilarity (b), as delimited by UPGMA hierarchical clustering of phylogenetic beta diversity ($p\beta_{sim}$) in 200×200 km grid cells, constraining the number of clusters to $k = 6$.

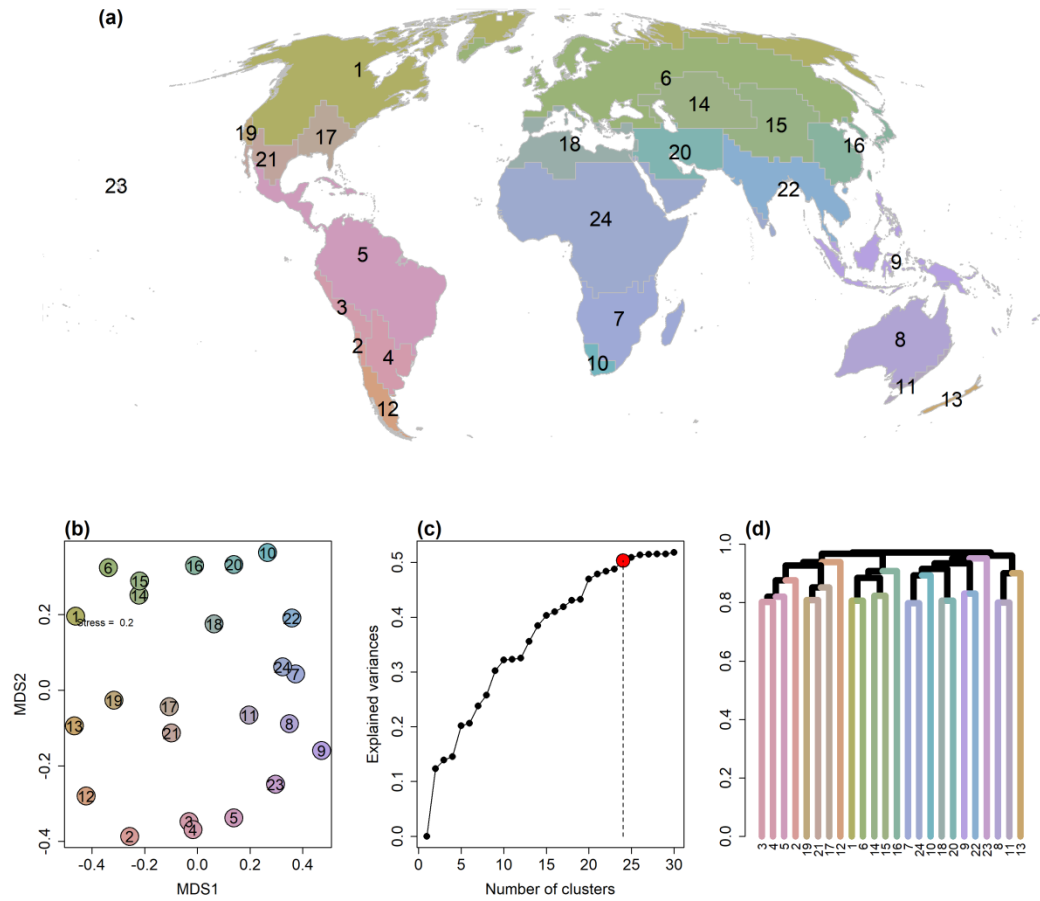
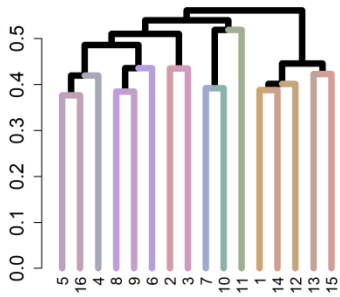
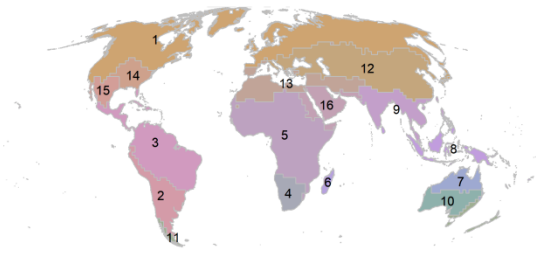


Figure S6. Map of the terrestrial taxonomically distinct phylogeographic units of the world (a), and their relationship presented as an NMDS ordination plot (b) and as a dendrogram of dissimilarity (d), as delimited by UPGMA hierarchical clustering of taxonomic beta diversity (β_{sim}) in 200×200 km grid cells. Grid cells cluster into 25 units based upon the ‘elbow’ method considering the range of explained variances (c). Colours differentiating between units in the NMDS plot, dendrogram and map are identical.

(a)



(b)

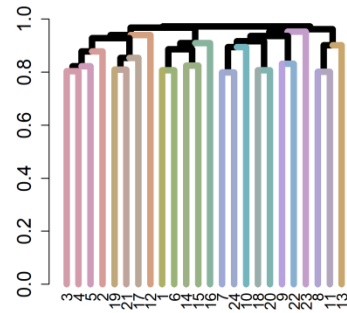
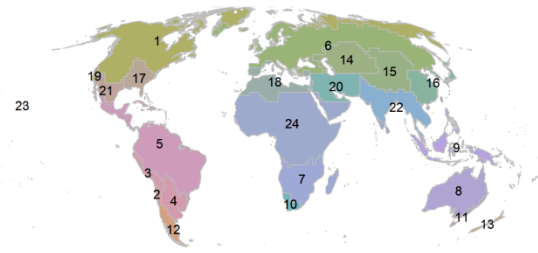


Figure S7. Maps of the terrestrial phylogenetic (a) and taxonomic (b) regionalisation of the world side by side.

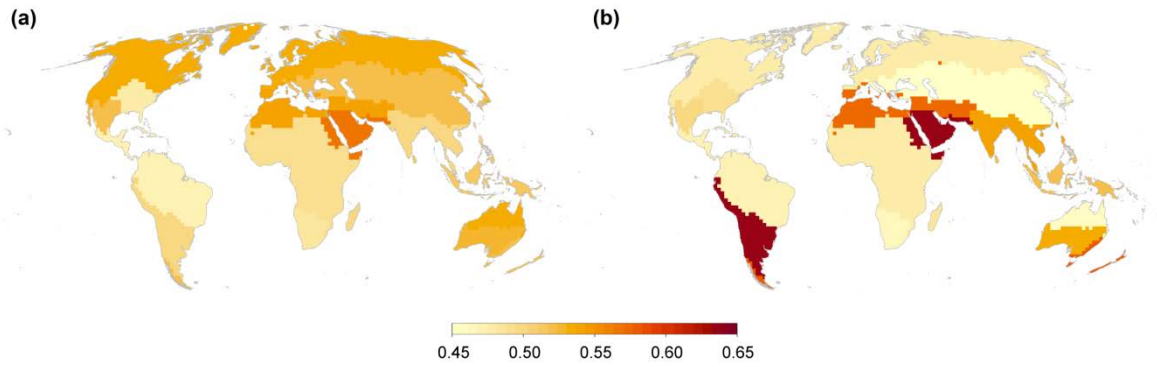


Figure S8. Evolutionary distinctiveness within the 16 phytogeographical units, considering only lycophytes and ferns (a) and gymnosperms (b), quantified as the mean of pairwise $p\beta_{\text{sim}}$ values between each unit, contrasted with all other units. Darker regions indicate regions of higher evolutionary distinctiveness.